Transactions of the **13th International Conference on Structural Mechanics in Reactor Technology** (SMiRT 13), Escola de Engenharia - Universidade Federal do Rio Grande do Sul, Porto Alegre, Brazil, August 13-18, 1995

Toughness of the austenitic cladding and its influence on the safety of a reactor pressure vessels

Schmitt, W., Hodulak, L., Sun, D.-Z.
Fraunhofer-Institut für Werkstoffmechanik, Freiburg, Germany

ABSTRACT: The behaviour of hypothetical cracks located in the ferritic base material beneath the austenitic cladding ist strongly influenced by the integrity of the cladding. In order to assess the toughness and the load carrying capacity of the cladding and its influence on initiation and propagation of the subclad crack a three-point bend test was performed with a test piece containing a semi-elliptical subclad crack. The test is analysed by damage mechanics concepts based on the Gurson model with material parameters determined from sub-sized tension tests.

1 INTRODUCTION

The criticality of hypothetical cracks located in the ferritic base material beneath the austenitic cladding ist strongly influenced by the integrity of the cladding: If the cladding is intact the crack tip loading, e.g. during an emergency core cooling accident is significantly reduced compared with the case where the cladding is assumed to be broken. Figure 1 shows the calculated J integral vs. temperature for an infinitely long circumferential crack of depth 30mm during a typical ECC transient with intact (solid) and broken (dashed) cladding.

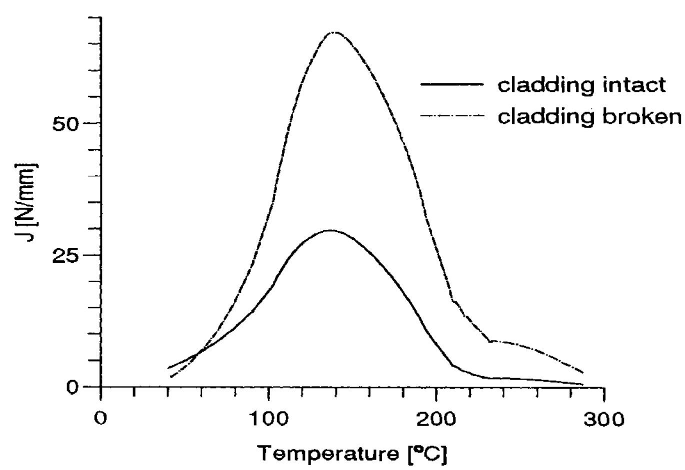

Figure 1: J-integral for a subclad crack during transient, intact and broken cladding

The assumption of a broken cladding might not be conservative with respect to maximum arrest crack depths, because due to the overestimation of the crack tip loads initiation would be predicted too early in the transient. Since at early times large parts of the vessel wall might still be at upper shelf temperatures the predicted arrest crack depth could be much smaller than in reality. The proper assessment of the load carrying capacity of the cladding is difficult since the application of the J-integral concept requires homogeneous material and the toughness gradients in the material are difficult to determine by standard test procedures. Therefore, an experiment was performed and analyzed with a cladded specimen containing a semi-elliptical flaw in the ferritic base material loaded under three-point bending.

2 TEST SET-UP AND MATERIAL CHARACTERIZATION

The specimen is made of the ferritic steel, German designation 20 MnMoNi 5 5 (ASTM A 508 Cl 3) with an austenitic cladding, dimensions 900 x 120 x (60 + 7) mm^3. Beneath the cladding a semi-elliptical surface crack 5 mm deep and 30 mm long had been fabricated in the base metal before the austenitic cladding was welded. The test was performed at room temperature where ductile material behaviour is prevailing in cladding and base material. Hence, the simulation of the test is performed on the basis of the modified Gurson model (Gurson 1977, Needleman and Tvergaard 1984) which had already been applied to the evaluation of fracture totughness of primary circuit steel components (Sun et al. 1992, Schmitt and Blauel 1993, Schmitt et al. 1994).

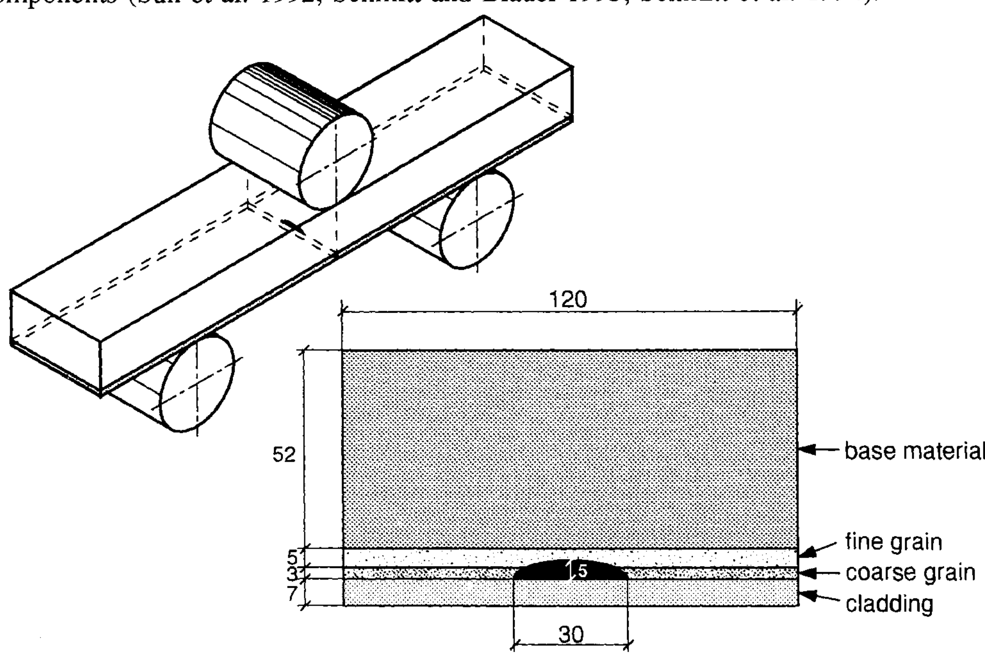

Figure 2: Test set-up and specimen geometry

Figure 2 shows a sketch of the specimen and of the test set-up. Due to the influence of the heat input during the welding process there is a gradient in the material properties between the unaffected base material and the cladding (taken into account by introducing a fine grain zone and a coarse grain zone). Sub-sized round bar tension specimens were taken from another representative block in order to characterize the different material zones by stress-strain curves and critical void volume fractions for the Gurson model. The validation of the Gurson parameters is achieved by comparing the measured and calculated J-resistance curves from four SENB (10 x 10)-specimens taken from different materials zones. From these tests and the corresponding numerical simulations the appropriate element sizes representing the characteristic material length were obtained.

3 RESULTS OF TEST AND SIMULATIONS

In two-dimensional pre-test calculations the crack was modelled as a through-crack, a region around the crack was in plane strain, the rest of the specimen in plane stress.

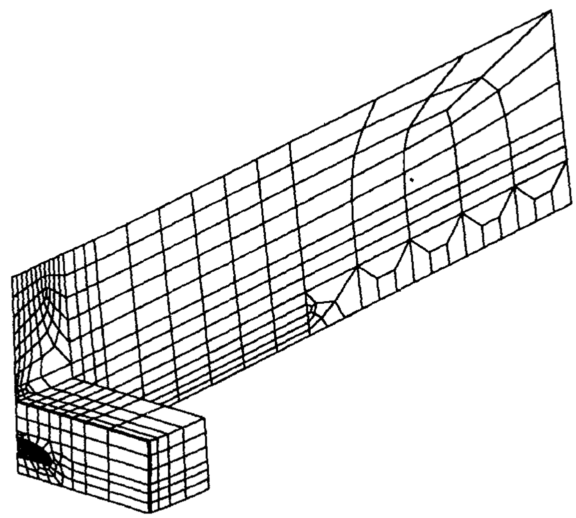

Figure 3: Combined 2D/3D finite element model

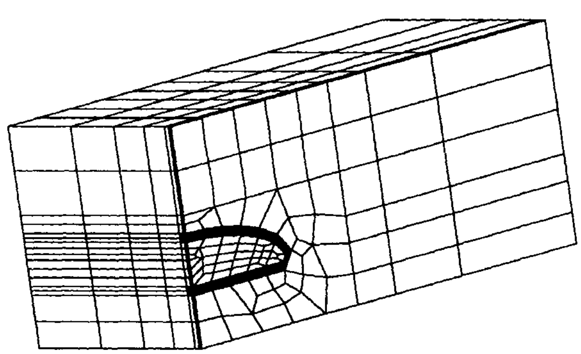

Figure 4: 3D-part of the finite element mesh containing the crack

These calculations predicted initiation in the cladding at a bending displacement of 4 mm and in the base material at 5 mm. In the experiment, initiation and extension were monitored by direct current potential, with probes in the cladding and in the base material, and by strain gauges attached above the crack on the cladding. Well before the final bending displacement of 24 mm all signals had given indications of crack propagation. After the test the numerical simulation was repeated using a reduced three-dimensional model as shown in figure 3. Here, only a region around the crack is modelled in 3D, the remaining specimen is modelled in plane stress. The proper transition between the plane and the volumetric parts of the mesh is ensured with constraint equations. The model has a total of 331 2D-elements, 1189 3D-elements and 6690 nodal points. Figure 4 shows a magnification of the 3D-part with the crack beneath the cladding in the base material.

Figure 5 shows the force vs. bending displacement diagram of the experiment together with the calculated curves. Both calculated curves are close together and give a rather good approximation to the experimental curve. However, at larger displacements crack extension especially in the cladding is overestimated by the two-dimensional simulation and the resulting force is increasingly underestimated. The three-dimensional model continues to match the experimental curve very well.

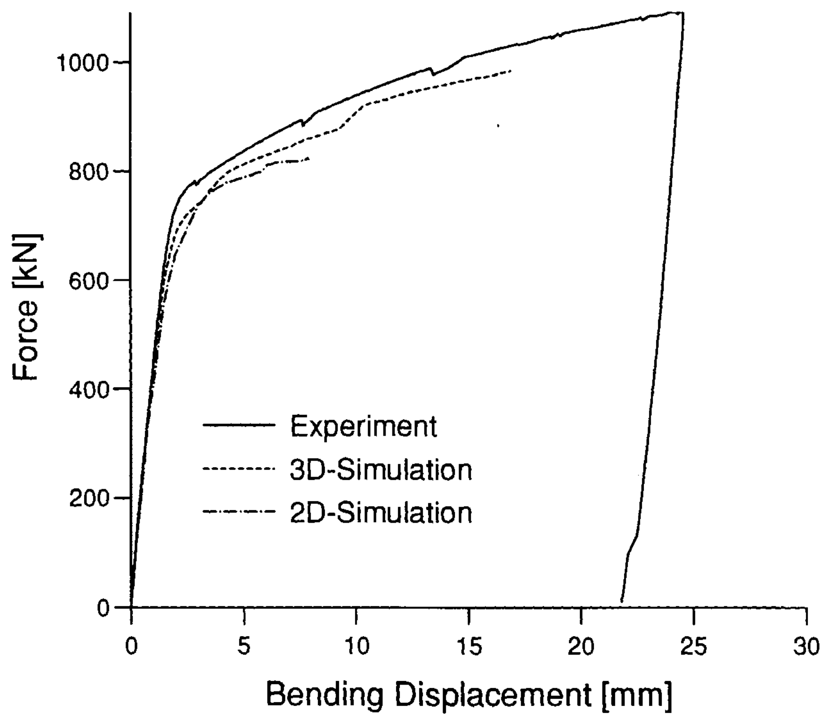

Figure 5: Measured and calculated (2D and 3D) forces vs. bending displacement

Figure 6 shows the calculated crack extension in the cladding and in the base material, evaluated at the deepest point of the crack for the three-dimensional model. According to the 3D-simulations crack initiation occured at about 3 mm bending displacement in

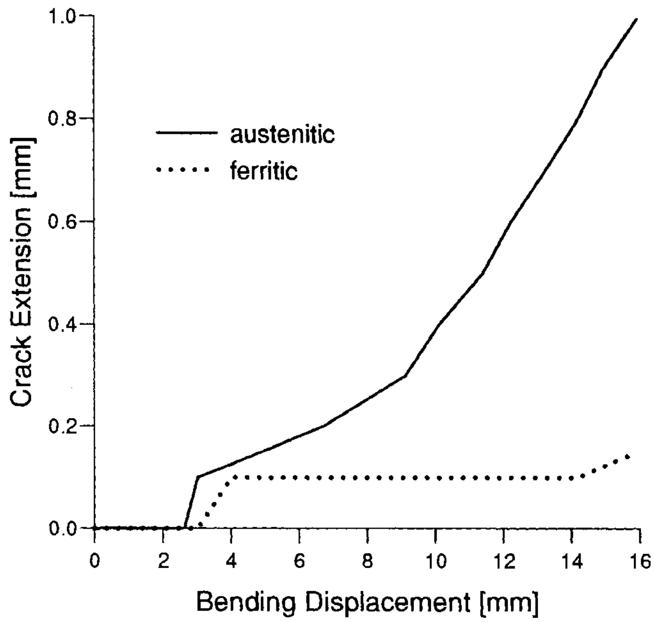

Figure 6: Calculated ductile crack extension in cladding and base material

cladding and a little later in the base material. However, the crack propagation takes place predominantly in the cladding. Significant crack extension in the base material seems to start only at bending displacements of about 14 mm. This is confirmed by the evaluation of the potential drop and of the strain gauge signal above the crack.

4 CONCLUSIONS

The integrity of the austenitic cladding above a subclad crack was demonstrated in a model experiment up to loads above general yield. These load levels can not be produced by thermal stresses as a consequence of Loss-of-Coolant-Accidents. Hence, the shielding effect of an intact cladding on the crack tip loads of subclad cracks may be taken into account for the evaluation of thermal shock transients. This paper gives a brief summary of this work, more details may be found in (Schmitt and Brocks 1994).

5 ACKNOWLEDGEMENT

The major part of this work has been supported by the German Minister for Research and Development under contract number 1500915.

6 REFERENCES

Gurson, A.L. 1977, Continuum theory of ductile rupture by void nucleation and growth: part I - yield criteria and flow rules for porous ductile media, J. Engng Mater.

Technol. 99, 2-15

Needleman, A. & Tvergaard, V. 1984, An analysis of ductile rupture in notched bars, Journal of the mechanics and physics of solids, Vol. 32, 461-490

Schmitt, W. & Brocks, W. 1994, Analyse und Weiterentwicklung bruchmechanischer Versagenskonzepte, Schwerpunkt: mikromechanische Materialmodelle, IWM-Bericht T 19/94

Schmitt, W. & Blauel, J.G. 1993, Application of micromechanical material models for the evaluation of fracture toughness of primary circuit steel components, Small Specimens Test Techniques Applied to Nuclear Reactor Vessel Thermal Annealing and Plant Life Extension, ASTM STP 1204, W.R. Corwin, F.M. Haggag, and W.L. Server, Eds., American Society for Testing and Materials, Philadelphia, 106-117

Schmitt, W., Sun, D.-Z, Böhme, W. & Nagel, G. 1994, Evaluation of fracture toughness based on results of instrumented Charpy tests, Int. J. Pres. Ves. & Piping 59, 21-29

Sun, D.-Z., Kienzler, R. Voss, B. & Schmitt, W. 1992, Application of micromechanical models to the prediction of ductile fracture, Fracture Mechanics: Twenty-Second Symposium (Volume II), ASTM STP 1131, S.N. Atluri, J.C. Newman, Jr., I.S. Raju, and J.S. Epstein, Eds., American Society for Testimg and Materials, Philadelphia, 368-378